Proceedings of the 11th World Congress on New Technologies (NewTech'25)
Paris, France - August, 2025
Paper No. ICBB 183
DOI: 10.11159/icbb25.183

Amperometric Detection of Creatinine as a Kidney Biomarker using a Laser-Induced Graphene- Based Non-enzymatic Biosensor

[1,2,5] Amany Attia, [1,4] Mohamed A. Ghazy, [2,3] Ahmed Abd Elmoneim
[1] Biotechnology Program, Faculty of Basic and Applied Science, Egypt-Japan University of Science and Technology, New Borg El Arab, Alexandria, 21934, Egypt; [2] Graphene Center of Excellence for Energy and Electronic Applications, Egypt-Japan University of Science and Technology, New Borg El Arab, Alexandria, 21934, Egypt; [3] Nanoscience Program, Faculty of Basic and Applied Science, Egypt-Japan University of Science and Technology, New Borg El Arab, Alexandria, 21934, Egypt; [4] Biochemistry Department, Faculty of Science, Ain Shams University, Cairo, 11566, Egypt; [5] Biochemistry Division, Chemistry Department, Faculty of Science, Tanta University, Tanta, 31527, Egypt.
[1] amany.attya@ejust.edu.eg ,[2] mohamed.ghazy@ejust.edu.eg , [3] ahmed.abdelmoneim@ejust.edu.eg

Abstract **-** Chronic kidney disease (CKD) represents a significant global health challenge, characterized by its high prevalence and insidious progression over extended periods. Creatinine, a significant metabolic byproduct of muscle metabolism, functions as a crucial biomarker for evaluating kidney function and facilitates the early detection and monitoring of chronic kidney disease (CKD). Electrochemical biosensors represent a promising approach for point-of-care testing of creatinine, facilitating continuous evaluation of kidney function. In this study, we present the development of a non-enzymatic amperometric biosensor for the detection of creatinine utilizing a laser-induced graphene (LIG) platform. LIG functions as an effective transducer for sensitive electrochemical measurements, attributed to its high electrical conductivity, extensive surface area, low manufacturing cost, and straightforward fabrication process. The electrode surface was modified using cuprous oxide–bovine serum albumin core-shell nanoparticles (Cu_2O–BSA NPs), serving as a stable electrocatalyst for the oxidation of creatinine. The morphology and size distribution of the as-prepared Cu_2O-BSA NPs were examined via transmission electron microscopy (TEM), while crystallographic structure and phase purity were confirmed using X-ray diffraction (XRD). The surface of the laser-induced graphene (LIG) electrode was analyzed using scanning electron microscopy (SEM) to assess its topology and porosity. The sensor's electrochemical performance was evaluated by chronoamperometry, facilitating accurate determination of current responses for creatinine detection at applied potentials. The amperometric measurements indicated a linear detection range of 10 μM to 5 mM, with a limit of detection (LOD) around 20 μM, highlighting the sensor's potential for clinically relevant creatinine monitoring.

Keywords**:** Creatinine, Cu_2O–BSA NPs, Laser-induced graphene, Non-enzymatic Amperometric Biosensor.

1. Introduction

Chronic Kidney Disease (CKD) is characterized by a progressive loss of kidney function over a long period; months or years, with a decline in glomerular filtration rate (GFR). It represents a significant global public health burden affecting over 10 % of adult population worldwide, with rising incidence due to aging populations, diabetes, and hypertension [1], [2]. For Egyptian population, 7.1 million individuals were estimated as CKD patients in 2017, and this number is expected to double by 2030 [3]. CKD is often asymptomatic in its early stages, making early diagnosis critical to prevent progression to end-stage renal disease (ESRD), which requires dialysis or transplantation [4].

Creatinine, a metabolic byproduct of creatine and phosphocreatine in muscle tissues, is widely used as a clinical biomarker to evaluate kidney function. Under normal conditions, creatinine is filtered from bloodstream by glomeruli of kidneys with relatively constant amount every day and then excreted in urine with no or minimal reabsorption [5], [6]. Elevated levels in blood indicate impaired renal clearance and are commonly used to estimate the GFR. Thus, monitoring creatinine is essential in the early detection and management of CKD [7].

Various analytical techniques have been employed to measure creatinine levels, including Jaffé colorimetric method [8], spectrophotometry [9], enzymatic assays [10], high-performance liquid chromatography (HPLC) [11], and electrophoresis [12]. Recently, electrochemical biosensors have emerged as a promising alternative for creatinine detection due to their high sensitivity, rapid response, cost-effectiveness, and suitability for miniaturization and point-of-care (POC) testing with minimal sample volume and preparation [13]. Among the various types of electrochemical sensors,

non-enzymatic biosensors have gained particular attention because they eliminate the stability issues associated with enzyme-based systems, such as denaturation and short shelf life [14], [15], [16].

In this study, we report the amperometric detection of creatinine using a novel non-enzymatic electrochemical biosensor based on laser-induced graphene (LIG) electrode modified with cuprous oxide-bovine serum albumin core-shell nanoparticles (Cu_2O-BSA NPs) via a simple drop-casting method [17], [18]. The LIG transducer, fabricated by direct laser scribing of polyimide film, offers a porous, highly conductive carbon structure ideal for sensor applications [19], [20]. Cuprous oxide is well-known for its electrocatalytic activity, especially towards creatinine oxidation. While BSA, as a globular protein, has an essential role in the stabilization of inorganic nanoparticles and their colloidal dispersion. The proposed Cu_2O-BSA/LIG electrode demonstrates a promising performance for creatinine measurements, offering facile and cost-effective fabrication process, as well as rapid and reliable detection.

2. Materials and Method

2.1. Materials

Creatinine (Techno Pharmchem, India), Albumin Bovin Fraction V (MP Biomedical, New Zealand), Ascorbic acid (SDFCL, India), Sodium hydroxide pellets, Copper nitrate trihydrate, and Ethanol absolute all from (Fisher chemical), DI water, Ethylene Glycol (Acros Organics), Polyimide sheets (PI 100 µm), silver conductive adhesive (Electron Microscopy Sciences), Disodium hydrogen phosphate (SDFCL, India), Potassium dihydrogen phosphate (Scharlau, Spain), Sodium chloride (K+S, US), Potassium chloride (Fisher chemical), and Hydrochloric acid for Phosphate Buffer Saline (PBS) preparation and pH adjustment.

2.2. LIG design and Fabrication

The LIG fabrication process utilized a Universal Laser System (VLS 3.50DT) equipped with a CO_2 laser source of a 10.6 µm wavelength, and a maximum power output of 50 watts. The LIG electrode pattern was designed utilizing CorelDRAW X5 software. Fig. 1 depicts the fabrication process of LIG electrodes. A PI sheet with a thickness of 100 µm was initially cleaned with ethanol and subsequently affixed to the processing area of the laser machine. The PI sheet was inscribed using CO_2 laser beam in a raster mode, following adjustments to the laser system settings, including laser power at 5%, scanning speed at 5%, and a pulse per inch (PPI) of 1000.

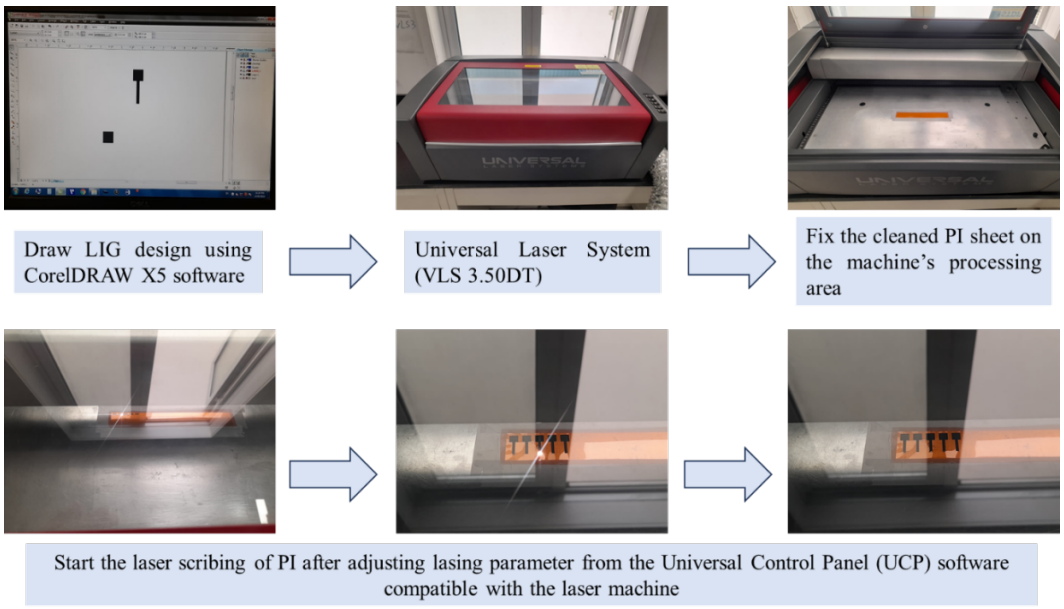

Fig. 1. LIG fabrication process. The diagram describes the fabrication of LIG using CO_2 laser scribing of PI sheet as a carbon rich material.

2.3. Preparation of Cu_2O-BSA NPs

Cu_2O-BSA NPs were synthesized by a facile chemical reduction method at room temperature as reported in previous work with some modifications [18]. Under magnetic stirring, 70 mg of BSA was dissolved in 26.4 ml DI water for 10 min. To this BSA solution, 1.4 ml (0.2 M) copper nitrate solution was added and stirred for 1 min before introducing 2.2 ml (1 M) NaOH under stirring for another 5 min. Then, Cu^{+2} ions were reduced by dropwise addition of 5 ml (0.1 M) A.A. After stirring for 10 min, the solution turned into a stable yellow-orange colloid, indicating the successful formation of Cu_2O-BSA NPs. The colloidal suspension was then allowed to stand undisturbed for 1 hr. and then centrifuged three times at 8000 rpm for 10 min to obtain a pellet of the as-synthesized Cu_2O-BSA NPs. The pellet was subsequently dried using a vacuum freeze dryer and stored at 4 °C in a well-sealed small brown glass bottle for future use.

2.4. Preparation of modified Cu_2O-BSA/LIG electrode

Cu_2O-BSA NPs were dispersed in a mixture of water, ethanol, and ethylene glycol; 70%:25%:5%, respectively, with a concentration of 1 mg/ml and ultrasonicated for 2 hr. A volume of 5 µL was then drop cast on the 5x5 mm^2 working area of the LIG electrode and left to completely dry at room temperature.

3. Results and Discussion

3.1. Structural and Morphological characterization of LIG

The surface morphology of pristine LIG electrode was investigated under scanning electron microscope (SEM, JSM-6360LA, JEOL, Japan) at various magnifications after coating for 15 min by Sputter coater (SPI-Sputter coater, USA), Fig. 2. At low magnification (60×), Fig. 2a, the SEM micrograph shows a well-defined layered structure with parallel features along the cross-section, indicative of the characteristic graphitic arrangement formed during the laser scribing process. This morphology suggests efficient graphitization and the formation of a continuous conductive network, which is essential for high electrochemical performance.

At higher magnifications (400x to 3000x), the SEM images demonstrate a highly porous, three-dimensional architecture with interconnected pores and a rough surface texture, Fig. 2(b-d). The porous structure becomes more obvious as the magnification increases, exposing a network of micro- and mesopores throughout the electrode surface. This porosity enhances the effective surface area and offers numerous active sites for Cu_2O loading and interaction with creatinine.

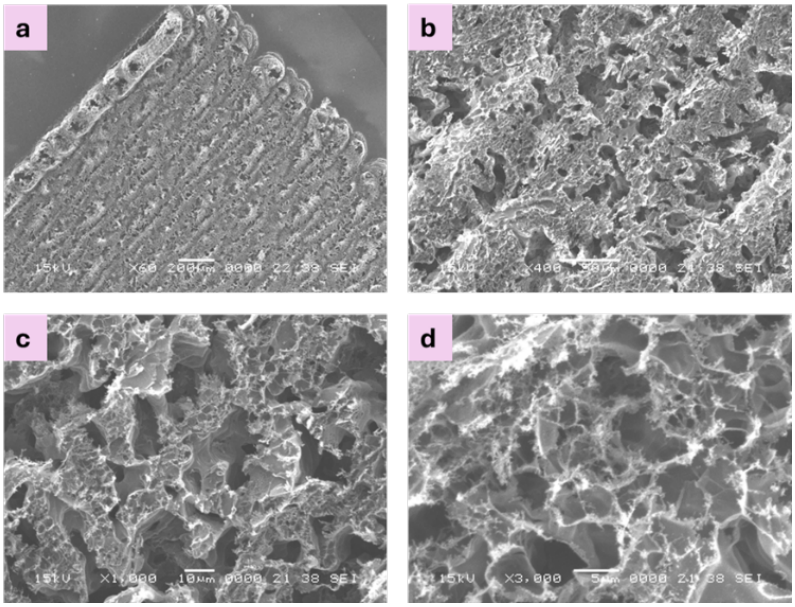

Fig. 2: SEM micrographs of pristine LIG. The surface morphology of pristine LIG was examined at different magnification powers of 60x (a), 400x (b), 1000x (c), and 3000x (d).

3.2. Structural and Morphological characterization of Cu_2O-BSA NPs

The morphological and structural characteristics of the as-synthesized Cu_2O-BSA nanoparticles were investigated using both transmission electron microscopy (TEM, JEOL JEM-2100F, Japan), and X-ray diffraction (Shimadzu XRD-6100, Japan) analysis, as illustrated in Fig. 3. Fig. 3a presents a TEM image of the as-synthesized Cu_2O–BSA NPs which are majorly spherical in shape and highly monodispersed, with standard deviation of 35.53 nm and an average particle size of 190.85 nm, as appeared in Fig. 3b. Fig. 3c of HRTEM indicates that the Cu_2O–BSA NPs exibit a core-shell structure with Cu_2O constituting the core part while the BSA protein forming the shell coating with approximately 5 nm thickness. The presence of BSA stabilizing shell also resulted in a well-defined interparticle separation, enhancing colloidal stability and biocompatibility of inorganic nanoparticles.

Figure 3d shows the crystallographic structure of Cu_2O-BSA NPs validated by XRD analysis (Xlab-6100, Shimadzu, Japan) at 40.0 (kV) and 30.0 (mA) operating voltage and current, respectively. The diffraction patterns were obtained for 2θ values between 5 and 80 degrees, with a scanning speed of 12.0000 (degrees/min). The diffraction pattern displays distinct peaks at 2θ values of 29.33, 36.22, 42.11, 61.25, and 73.39, corresponding to the (110), (111), (200), (211), and (220) planes, respectively. These values align closely with the standard reference pattern for cubic-phase Cu_2O (JCPDS No. 65-3288) [18]. The sharp and intense nature of the peaks indicates high crystallinity of the synthesized Cu_2O–BSA NPs.

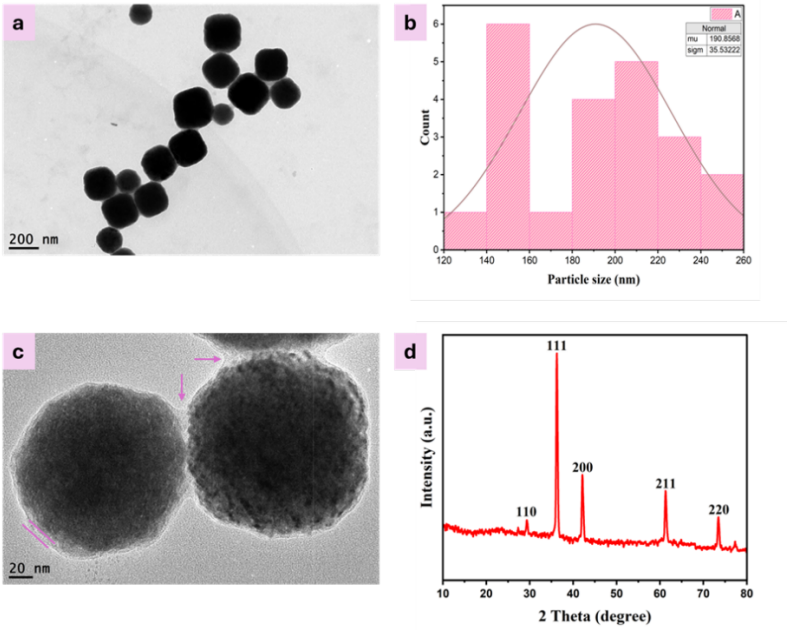

Fig. 3. Structural and morphological characterization of Cu_2O-BSA NPs, showing TEM image (a), Particle size distribution graph (b), HRTEM (c), and XRD pattern of Cu_2O-BSA NPs (d).

3.3. Amperometric measurements of modified Cu_2O-BSA/LIG electrode

Chronoamperometry was conducted for the electrochemical characterization of Cu_2O-BSA-modified LIG electrode for creatinine measurements. All electrochemical measurements were performed using VersaSTAT 4 (AMETEK Scientific) workstation with conventional electrochemical cell composed of Cu_2O-BSA-modified LIG as a working electrode, Ag/AgCl as a reference electrode, and a platinum wire as a counter electrode. Amperometric measurements were performed in 10 mM PBS (pH 7.4) containing a fixed creatinine concentration of 1 mM, while varying the applied potential. The current response was recorded after 5 s for each applied potential. For background signal, the current response of 10 mM PBS without creatinine was also measured. The optimized potential was determined by plotting the signal to background current ratio

against applied potentials. From fig. 4b, the potential of 0.1 V exhibited the highest S/B ratio; thus, it was selected as optimized potential for subsequent measurements.

To evaluate the analytical performance of the proposed electrode towards creatinine sensing, amperometric measurements were made at different creatinine concentrations, from 10 µM to 5 mM in 10 mM PBS, under optimized potential of 0.1 V (vs. Ag/AgCl), Fig. 5a. Calibration plots for creatinine were constructed using amperometric current responses measured at 5 s. As shown in Fig. 5(b-c), the current response increased as a function of creatinine concentration, and the modified electrode showed a linear trend over both, the low concentration range of 10 µM–400 µM and the high concentration range of 1.0 mM–5.0 mM with a correlation coefficient of 0.99 and 0.985, respectively. The analytical performance of the proposed electrode presents a wider linear range and a limit of detection (LOD) of approximately 20 µM.

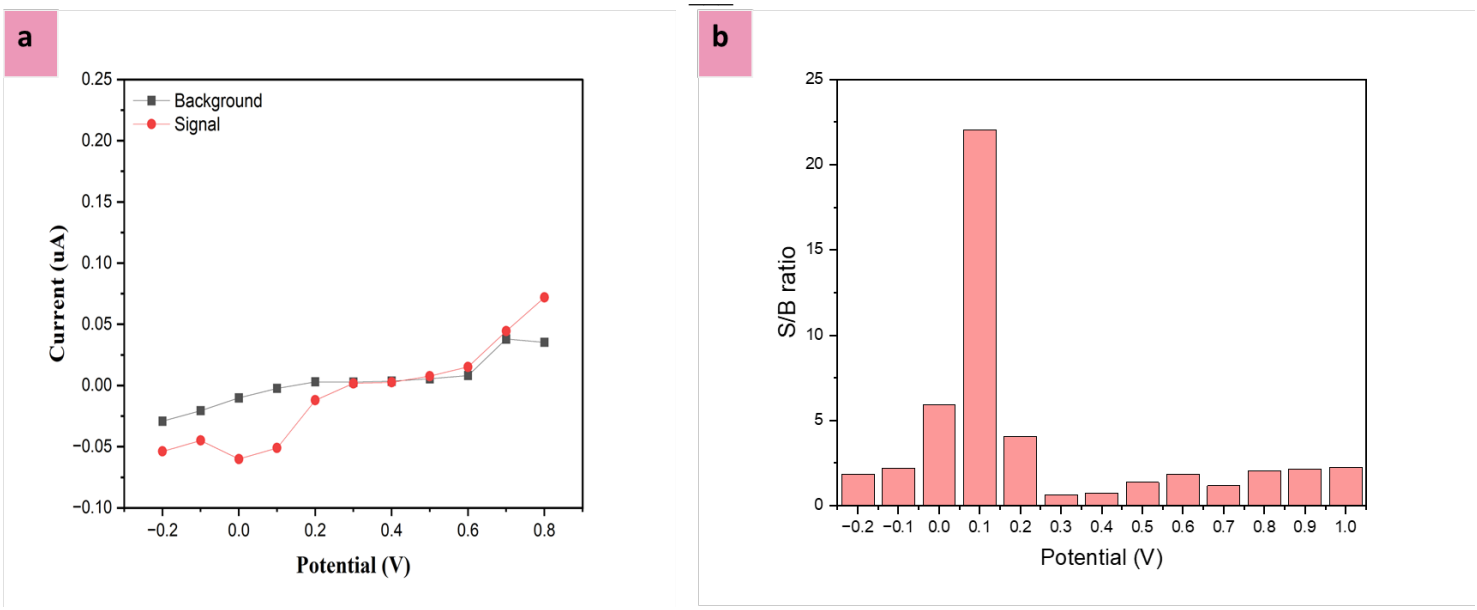

Fig. 4. (a) Amperometric current response of 10 mM PBS (pH 7.4) with 1 mM creatinine (red line) and without creatinine (black line) at 5 s sampling time, while (b) is the S/B current ratio extracted from the data of (a) at different applied potential.

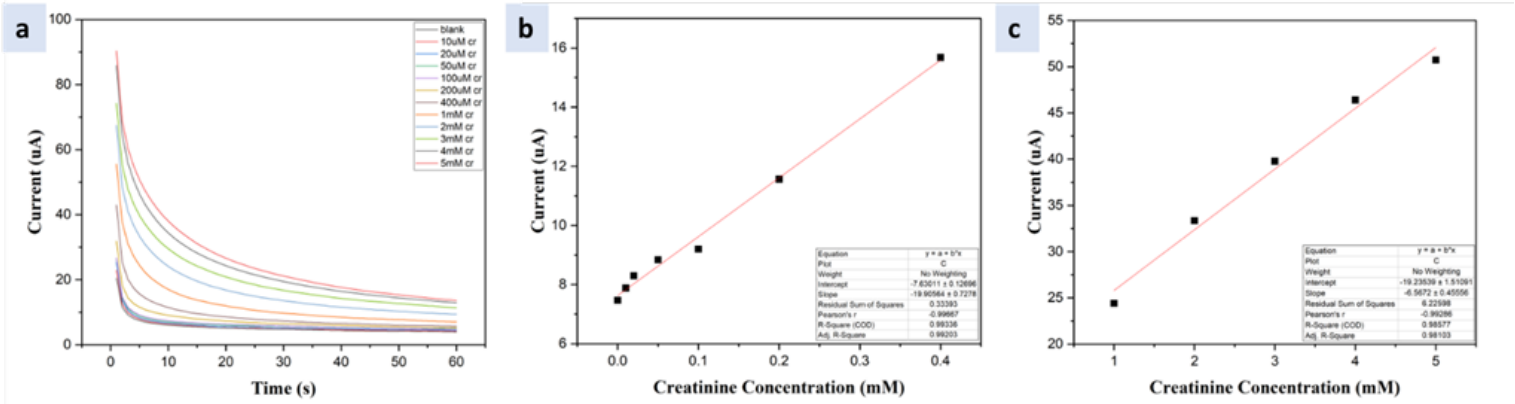

Fig. 5: Amperometric measurements on Cu_2O-BSA/LIG electrode with varying creatinine concentrations (10 µM to 5.0 mM) in 10 mM PBS (pH 7.4) at 0.1 V against Ag/AgCl for 60 s (a). Fig. 5(b-c) shows creatinine detection calibration plots from signal measurements in (a).

4. Conclusion

In this work, LIG electrodes were fabricated by CO2 laser engraving of PI sheet resulting in highly porous structure offering large surface area for electrocatalyst loading and interaction with creatinine. The electroactive material of Cu_2O-BSA NPs were synthesized by a simple chemical reduction method at room temperature. The resulting sphere NPs exhibit an average size of 190 nm and demonstrate good monodispersity. The as-prepared Cu_2O-BSA NPs dispersion was used to modify the surface of LIG working electrode. Chronoamperometry demonstrated that Cu_2O-BSA NPs exhibit direct electrocatalytic activity for the oxidation of creatinine in 10 mM PBS at a potential of 0.1 V. The developed sensing electrode facilitated the detection of creatinine, achieving LOD of approximately 20 μM and a linear detection range from 10 μM to 5.0 mM. Consequently, Cu_2O-BSA NPs are expected to serve as effective nanostructures for the development of non-enzymatic electrochemical creatinine sensing devices.

Acknowledgements

The authors would like to show their gratitude to the Missions Sector-Ministry of Higher Education (MOHE) and the Japan International Cooperation Agency (JICA) for supporting the MSc scholarship of the first author at Egypt-Japan University of Science and Technology (E-JUST).

References

[1] D. Desai, A. Kumar, D. Bose, and M. Datta, "Ultrasensitive sensor for detection of early stage chronic kidney disease in human," *Biosens. Bioelectron.*, vol. 105, pp. 90–94, May 2018, doi: 10.1016/j.bios.2018.01.031.

[2] Y. Dong, Y. Liu, J. Lv, L. Yang, and Y. Cui, "Advancements in Amperometric Biosensing Instruments for Creatinine Detection: A Critical Review," *IEEE Trans. Instrum. Meas.*, vol. 72, pp. 1–15, 2023, doi: 10.1109/TIM.2023.3279459.

[3] M. Gawad, N. Yousri, and M. Hammad, "Renal registry for chronic kidney disease patients in Egypt: causes and comorbidities, data from a private clinic in an urban area," *J. Egypt. Soc. Nephrol. Transplant.*, vol. 24, no. 1, p. 54, 2024, doi: 10.4103/jesnt.jesnt_21_23.

[4] K. Hazarika, J. C. Dutta, and H. R. Thakur, "Clinical Analysis and Detection of Creatinine by Conventional Methods and Electrochemical Biosensors: A Review," *IEEE Sens. J.*, vol. 24, no. 1, pp. 16–27, Jan. 2024, doi: 10.1109/JSEN.2023.3332131.

[5] S. Bajpai, G. R. Akien, and K. E. Toghill, "An alkaline ferrocyanide non-enzymatic electrochemical sensor for creatinine detection," *Electrochem. Commun.*, vol. 158, p. 107624, Jan. 2024, doi: 10.1016/j.elecom.2023.107624.

[6] R. K. Rakesh Kumar, M. O. Shaikh, A. Kumar, C.-H. Liu, and C.-H. Chuang, "Zwitterion-Functionalized Cuprous Oxide Nanoparticles for Highly Specific and Enzymeless Electrochemical Creatinine Biosensing in Human Serum," *ACS Appl. Nano Mater.*, vol. 6, no. 3, pp. 2083–2094, Feb. 2023, doi: 10.1021/acsanm.2c05020.

[7] Z. Saddique, M. Faheem, A. Habib, I. UlHasan, A. Mujahid, and A. Afzal, "Electrochemical Creatinine (Bio)Sensors for Point-of-Care Diagnosis of Renal Malfunction and Chronic Kidney Disorders," *Diagnostics*, vol. 13, no. 10, p. 1737, May 2023, doi: 10.3390/diagnostics13101737.

[8] S. Nur Ashakirin, M. H. M. Zaid, M. A. S. M. Haniff, A. Masood, and M. F. Mohd Razip Wee, "Sensitive electrochemical detection of creatinine based on electrodeposited molecular imprinting polymer modified screen printed carbon electrode," *Measurement*, vol. 210, p. 112502, Mar. 2023, doi: 10.1016/j.measurement.2023.112502.

[9] K. Karn-orachai and A. Ngamaroonchote, "Role of polyelectrolyte multilayers over gold film for selective creatinine detection using Raman spectroscopy," *Appl. Surf. Sci.*, vol. 546, p. 149092, Apr. 2021, doi: 10.1016/j.apsusc.2021.149092.

[10] G. Alvarez Menendez, O. Amor-Gutierrez, A. Costa Garcia, M. Funes-Menendez, C. Prado, D. Miguel, P. Rodriguez-Gonzalez, A. Gonzalez-Gago, and J. I. Garcia Alonso, "Development and evaluation of an electrochemical biosensor for creatinine quantification in a drop of whole human blood," *Clin. Chim. Acta*, vol. 543, p. 117300, Mar. 2023, doi: 10.1016/j.cca.2023.117300.

[11] D. Tsikas, A. Wolf, A. Mitschke, F.-M. Gutzki, W. Will, and M. Bader, "GC–MS determination of creatinine in human biological fluids as pentafluorobenzyl derivative in clinical studies and biomonitoring: Inter-laboratory comparison in

urine with Jaffé, HPLC and enzymatic assays," *J. Chromatogr. B*, vol. 878, no. 27, pp. 2582–2592, Oct. 2010, doi: 10.1016/j.jchromb.2010.04.025.

[12] O. B. de Oliveira Moreira, J. C. Queiroz de Souza, J. M. Beraldo Candido, M. P. do Nascimento, P. R. Chellini, L. M. de Lemos, and M. A. L. de Oliveira,"Determination of creatinine in urine and blood serum human samples by CZE-UV using on-column internal standard injection," *Talanta*, vol. 258, p. 124465, June 2023, doi: 10.1016/j.talanta.2023.124465.

[13] R. K. Rakesh Kumar, M. O. Shaikh, and C.-H. Chuang, "A review of recent advances in non-enzymatic electrochemical creatinine biosensing," *Anal. Chim. Acta*, vol. 1183, p. 338748, Oct. 2021, doi: 10.1016/j.aca.2021.338748.

[14] R. K. R. Kumar, A. Kumar, M. O. Shaikh, C.-Y. Liao, and C.-H. Chuang, "Enzymeless electrochemical biosensor platform utilizing Cu2O-Au nanohybrids for point-of-care creatinine testing in complex biological fluids," *Sens. Actuators B Chem.*, vol. 399, p. 134787, Jan. 2024, doi: 10.1016/j.snb.2023.134787.

[15] P. Singh, S. Mandal, D. Roy, and N. Chanda, "Facile detection of blood creatinine using binary Copper- Iron oxide and rGO-based nanocomposite on 3-D printed Ag-electrode under POC settings".

[16] C. L. Gonzalez-Gallardo, N. Arjona, L. Álvarez-Contreras, and M. Guerra-Balcázar, "Electrochemical creatinine detection for advanced point-of-care sensing devices: a review," *RSC Adv.*, vol. 12, no. 47, pp. 30785–30802, 2022, doi: 10.1039/D2RA04479J.

[17] G. Nkamuhebwa, A. A. El-Moneim, H. A. Ali Hassan, T. Tsuchiya, and M. A. Hassan, "Optimizing Lasing Parameters for Fabricating an Efficient Flexible Electrothermal Heater Based on Laser-Induced Graphene," *Mater. Sci. Forum*, vol. 1127, pp. 73–80, Sept. 2024, doi: 10.4028/p-KCJAn4.

[18] Z. Dai, A. Yang, X. Bao, and R. Yang, "Facile Non-Enzymatic Electrochemical Sensing for Glucose Based on Cu2O–BSA Nanoparticles Modified GCE," *Sensors*, vol. 19, no. 12, p. 2824, June 2019, doi: 10.3390/s19122824.

[19] T. S. D. Le, H. P. Phan, S. Kwon, S. Park, Y. Jung, J. Min, B. J. Chun, H. Yoon, S. H. Ko, S. W. Kim, and Y. J. Kim, "Recent Advances in Laser-Induced Graphene: Mechanism, Fabrication, Properties, and Applications in Flexible Electronics," *Adv. Funct. Mater.*, vol. 32, no. 48, p. 2205158, Nov. 2022, doi: 10.1002/adfm.202205158.

[20] T. Han, A. Nag, R. Simorangkir, N. Afsarimanesh, H. Liu, S. C. Mukhopadhyay, Y. Xu, M. Zhadobov, and R. Sauleau, "Multifunctional Flexible Sensor Based on Laser-Induced Graphene," *Sensors*, vol. 19, no. 16, p. 3477, Aug. 2019, doi: 10.3390/s19163477.